available at www.sciencedirect.com

ScienceDirect

journal homepage: www.elsevier.com/locate/ecolmodel

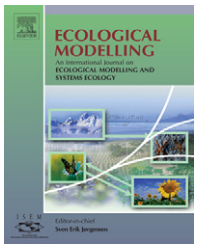

The importance of spawning season on the growth of Pacific saury: A model-based study using NEMURO.FISH

Daiki Mukai[a,*], *Michio J. Kishi*[b,c], *Shin-ichi Ito*[d], *Yutaka Kurita*[d]

[a] *Graduate School of Environmental Science, Hokkaido University, N10W5 Kita-ku, Sapporo, Hokkaido 060-0810, Japan*
[b] *Faculty of Fisheries Sciences Hokkaido University, c/o Chotatsuka, Hokkaido University, N13 W8, Sapproro 060-0813, Japan*
[c] *Ecosystem Change Research Program, Frontier Research Center for Global Change, 3173-25, Showa-machi, Kanazawa-ku, Yokohama 236-0001, Japan*
[d] *Tohoku National Fisheries Research Institute, Fisheries Research Agency, 3-27-5 Shinhama-cho, Shiogama, Miyagi 985-0001, Japan*

ARTICLE INFO

Article history:
Published on line 20 November 2006

Keywords:
Pacific saury
Bioenergetics model
Ecosystem model
NEMURO
NEMURO.FISH

ABSTRACT

NEMURO.FISH was applied to Pacific saury to study the dependence of spawning season on growth. The model was composed of three ocean domains, which corresponded to the Kuroshio, the Oyashio, and the interfrontal zone (mixed water) regions. In these three domains, a lower trophic model (NEMURO) was coupled with a simple physical model, and the time-variation of three zooplankton size classes was input as prey densities into the saury bioenergetics model. Three numerical experiments were examined using this model, which corresponded to three different spawning seasons. Results showed that in the first year winter-spawned saury showed the fastest growth, and spring-spawned showed the slowest growth, while in the second year (time to grow to 120 g wet weight), the reverse occurred, i.e., spring-spawned saury showed the fastest growth. This difference in growth, which depends on the spawning season, can explain the bimodal size distribution of early autumn catch data.

1. Introduction

Pacific saury (*Cololabis saira*) is an important pelagic commercial fish in the northwestern Pacific and the average total catch of saury is about 250,000 tonnes (t). Saury spawning starts in the mixed water region (the Kuroshio–Oyashio interfrontal zone) in autumn, moves to the Kuroshio region (the subtropical region) in winter and shifts back to the mixed water region in spring (Odate, 1977; Watanabe and Lo, 1989; Watanabe et al., 1997; Ito et al., 2004). Juveniles are advected to the Kuroshio extension region, then grow and migrate to the Oyashio region (the subarctic region) through the mixed water region for feeding. After sufficient feeding, they migrate back to the Kuroshio region to spawn. The knob length (KL, nearly the same as body length) of saury reaches 30 cm in adults and many studies have estimated the growth rate of saury using otolith analyses (Suyama et al., 1996; Oozeki and Watanabe, 2000). A recent fish bioenergetics model (Ito et al., 2004) used parameter sets derived from otolith analyses. They used a bioenergetics model coupled with a lower trophic model (NEMURO (North Pacific Ecosystem Model for Understanding Regional Oceanography); Kishi et al., 2007) and analyzed the influence of climate change on the growth of Pacific saury. Their model was composed of three oceanic domains (hereafter called boxes) corresponding to the Kuroshio (KR), the Oyashio (OY), and the interfrontal zone (mixed water regions) (MW), and showed that the surface heating or cooling in MW has the most influence on the change in Pacific saury growth rate. Warming in

* *Corresponding author*. Tel.: +81 11 706 5313; fax: +81 11 706 5313.
E-mail address: dmukai@ees.hokudai.ac.jp (D. Mukai).
0304-3800/$ – see front matter © 2006 Elsevier B.V. All rights reserved.
doi:10.1016/j.ecolmodel.2006.08.022

MW results in a reduction of zooplankton density and slows the growth of saury. The effect of warming in OY shows the same effect on saury growth rate, whereas, warming in KR accelerates the loss of saury weight.

The life history of Pacific saury is complicated and it has been difficult to clearly identify the mechanisms that determine variations in biomass and size-composition. Recent work by Kurita et al. (2004) estimated the hatch date of large Pacific saury and, combined with the information of the growth of the saury with no hyaline zone (Okuda, 2002), built a new life history scenario. According to Kurita's new scenario, saury, which is born early (autumn and winter), spawn in the first winter and also in the second winter. However, later (spring) spawned saury do not spawn in the first year, but do spawn in the second year.

Oozeki et al. (2004) and Oozeki and Watanabe (2000) showed that sea surface temperature (SST) and food density affect larval growth during early stages and SST and chlorophyll become more important in later stages. But the environmental influences on young and adult saury have not been quantified because saury is very sensitive and difficult to rear in laboratories. Although the life span of Pacific saury is unclear, Kosaka (2000) showed that two peaks in the size distribution can be found in early-autumn catch-data (right hand side of Fig. 7) and that these two peaks might be proof that the Pacific saury life span is about 2 years, considering that each peak corresponds to one main spawning season per year. Suyama et al. (2006) also revealed that Pacific saury consists of only 2-year-classes and the large-sized group (<29.0 cm) is considered to almost correspond to the age 1 fish group, while the medium- (24.0–29.0 cm) and small-sized groups (20.0–24.0 cm) almost correspond to the age 0 fish group.

In this paper, we improved the NEMURO.FISH model of Ito et al. (2004) and applied the model to three different spawning seasons. Our goal was to use the model to reproduce a reasonable time dependent growth curve of Pacific saury, which depended on spawning season. We performed three numerical experiments using this coupled model to answer the following questions: how do differences in spawning season affect saury growth? and how are bi-modal size distributions of catch data formed?

2. The fish bioenergetics/ecosystem coupled model

The basic model of the fish bioenergetics/ecosystem coupled model is NEMURO.FISH (NEMURO For Including Saury and Herring; Megrey et al., 2007). The NEMURO.FISH model was applied to saury life-history characteristics follows the approach described by Ito et al. (2004). NEMURO was applied to a three-box ocean model, where each box represents the KR, the MW and the OY region, respectively. In each box, SST was provided as the surface boundary condition and the mixed layer temperature was defined by SST (Fig. 1). SST is the highest in late August and lowest in late February (Fig. 6c of Ito et al., 2004). Temperature at the bottom of the mixed layer (BLT) was set to be constant and was given as the bottom boundary condition defined from the data of the World Ocean Atlas (Antonov et al., 1998). Bottom boundary conditions for temperature and nutrients in NEMURO are given in Table 1. The thickness of the mixed layer is increased (decreased) when the SST is lower (higher) than BLT although the mixed layer thickness could not be less than 30 m. The exchange rate of NO_3 and $Si(OH)_4$ between the mixed layer and the bottom layer was changed as a function of stability defined by the difference in temperature between SST and BLT. NEMURO was driven by SST forcing and light intensity at the surface. Small (ZS), large (ZL) and predatory (ZP) zooplankton densities and seawater temperature derived from NEMURO were used to couple with the Pacific saury bioenergetics model. Parameters used in the saury version of NEMURO.FISH are basically the same reported in Ito et al. (2004) except for a_c (the intercept for C_{MAX}, maximum consumption rate) and b_c (the slope of the allometric mass function for consumption). The value a_c is changed from 0.6 (cf. Table 2 of Ito et al., 2004) to 0.54 and the value b_c is changed from −0.340 (cf. Table 2 of Ito et al., 2004) to −0.256 because these values gave more reasonable results compared to observed data.

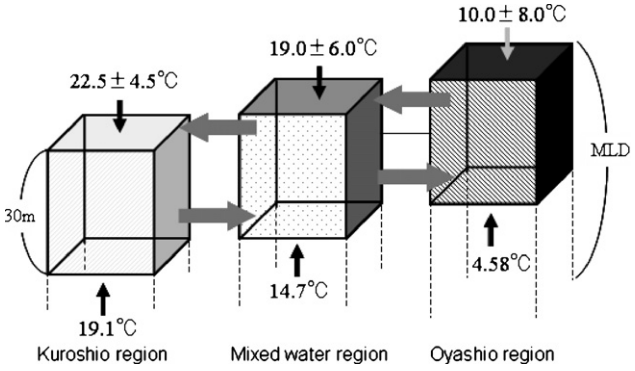

Fig. 1 – Schematic view of the three oceanographic domains. Each domain represents the Kuroshio, the mixed water and the Oyashio region, respectively. In each domain, SST is provided as the surface boundary condition (the numbers shown above each box are the annual mean and amplitude of SST) and the mixed layer temperature is defined by the SST. The temperature at the bottom of the mixed layer (the number shown beneath each box are the bottom temperature) is constant and given as the bottom boundary condition.

Table 1 – Bottom boundary conditions for temperature and nutrients in NEMURO

Bottom boundary condition	Kuroshio	Mixed water region	Oyashio
Water temperature (°C)	19.10	14.70	4.58
Nitrate (mol N l^{-1})	6.0×10^{-6}	18.0×10^{-6}	25.0×10^{-6}
Silicate (mol Si l^{-1})	6.0×10^{-6}	25.0×10^{-6}	30.0×10^{-6}

3. Material and methods

3.1. *Spawning season and area*

We divided the spawning season into three periods, autumn, winter and spring. In our model, the birth-date and spawning

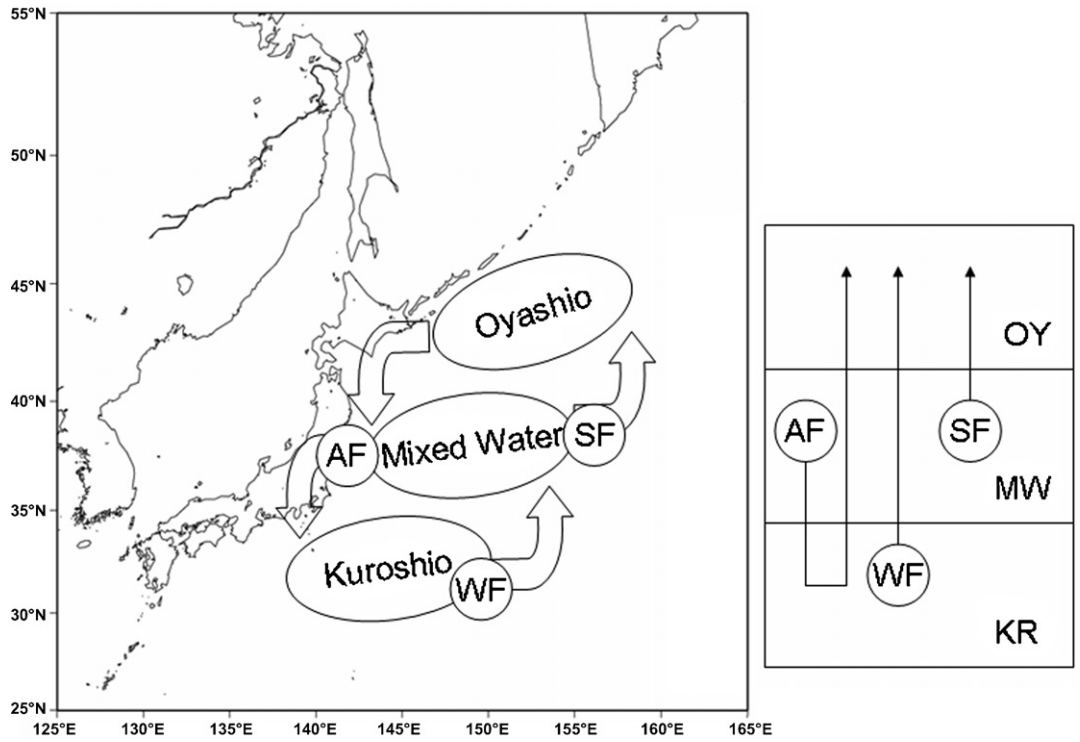

Fig. 2 – Schematic view of saury migration trajectories. The three oceanic domains correspond to the Kuroshio (KR), mixed water (MW), and the Oyashio (OY) regions. Autumn-spawned saury (AF) migrate from the MW region to the KR region, and again to the MW region and the OY region. Winter-spawned saury (WF) migrate from the KR region to the OY region through the MW region, while spring-spawned saury (SF) migrate northward from the MW region to the OY region. After sufficient feeding, AF, WF and SF migrate back to the KR region to spawn.

area of autumn-spawned saury (AF) were 15th October and the MW region, those of winter-spawned saury (WF) were 15th January and the KR region, and those of spring-spawned saury (SF) were 15th April and the MW region, respectively. The life span of saury was assumed to be 2 years and 1 month (1 month was added in order to express the second year egg production of AF) following Suyama et al. (1996). AF migrated from the MW to the KR region, and again to the MW and the OY region. WF migrated from the KR to the OY through the MW region, while SF migrated northward from the MW to the OY region (Fig. 2). After sufficient feeding, AF, WF and SF migrated back to the KR region to spawn. Table 2 shows vulnerability coefficients and half saturation constants for the saury bioenergetics models for AF, WF and SF, respectively.

It was assumed that saury spawn for up to 60 days depending on their KL. The ability to spawn was restricted to saury longer than 25 cm KL. The spawning beginning date depends on the KL (Kosaka, 2000), with longer fish spawning earlier. Fig. 3 describes this criterion. Spawning started from 15th September for saury longer than 34 cm KL. The start date of the spawning was defined by the KL as

$$\text{start date (date from September 15)} = \frac{180}{(25-34)(\text{KL (cm)}-34)} \quad (1)$$

and the duration was assumed to be 60 days. For instance, a 32 cm fish begins spawning on 25th October and continues to spawn until 23rd December while 27 cm fish begins to spawn on 2nd February and continues to spawn until 3rd March. Kurita (2006) suggested that spawning activity is reduced after spring, therefore, we defined the latest spawning start date to be 15th March and after 13th May, saury ceased to spawn.

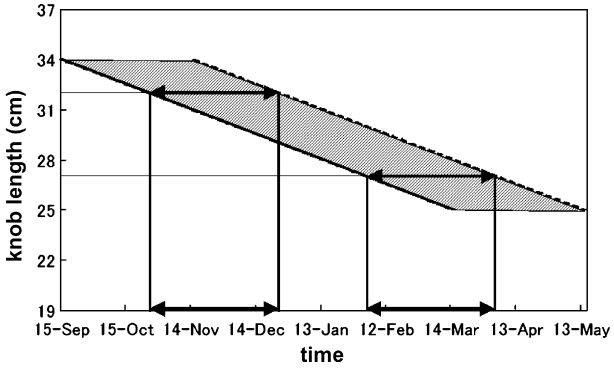

Fig. 3 – The spawning season criterion. The vertical axis shows knob length (KL, cm) and the horizontal axis shows date. The solid thick diagonal line shows the spawning start date, the broken thick diagonal line shows the spawning end date and the shaded area shows the spawning season. For example, a 32 cm fish begins spawning on 25th October and continues to spawn until 23rd December while a 27 cm fish begins to spawn on 2nd February and continues to spawn until 3rd March.

Table 2 – Saury bioenergetics model vulnerability coefficients and half saturation constants by saury life stages and spawning area for autumn (AF), winter (WF) and spring (SF) spawned saury, respectively

Stage	Half saturation constant, K_{ij}	Autumn-spawned saury (AF)				Winter-spawned saury (WF)				Spring-spwned saury (SF)			
		Area	Vulnerability, v_{ij}			Area	Vulnerability, v_{ij}			Area	Vulnerability, v_{ij}		
			ZS	ZL	ZP		ZS	ZL	ZP		ZS	ZL	ZP
1	0.1	MW	1.0	0.0	0.0	KR	1.0	0.0	0.0	MW	1.0	0.0	0.0
2	0.3	KR	1.0	0.0	0.0	MW	1.0	1.0	0.0	OY	1.0	1.0	0.0
3	0.6	MW	0.0	1.0	1.0	OY	0.0	1.0	1.0	MW	0.0	1.0	1.0
4	0.6	OY	0.0	1.0	1.0	MW	0.0	1.0	1.0	KR	1.0	0.0	1.0
5	0.6	MW	0.0	1.0	1.0	KR	1.0	0.0	1.0	MW	0.0	1.0	1.0
6	0.6	KR	1.0	0.0	1.0	MW	0.0	1.0	1.0	OY	0.0	1.0	1.0
7	0.6	MW	0.0	1.0	1.0	OY	0.0	1.0	1.0	MW	0.0	1.0	1.0
8	0.6	OY	0.0	1.0	1.0	MW	0.0	1.0	1.0	KR	1.0	0.0	1.0
9	0.6	MW	0.0	1.0	1.0	KR	1.0	0.0	1.0	MW	0.0	1.0	1.0

KR: Kuroshio water region; MW: mixed water region; OY: Oyashio water region; ZS: small zooplankton; ZL: large zooplankton; ZP: predatory zooplankton.

3.2. *Migration criteria*

Kosaka (2000) suggested that longer fish begin migrating northward earlier than shorter fish. Fukushima (1979) also suggested that longer fish begin migrating southward from the OY to the MW region earlier than shorter ones. For migration criteria from the MW to the KR region, we assumed the same movement criteria for movement from the OY to the MW region. Fukushima (1979) did not suggest a criterion for movement between the MW to the KR region. These criteria make it clear that larger fish can migrate across sharper temperature gradients. The rules defining time and temperature-dependent migration criteria are described below.

3.2.1. *Northward (feeding) migration (Kosaka, 2000)*

From the KR to the MW region: after 1st February, when the MW water temperature becomes higher than 15 °C, then saury migrates from the KR to the MW region, otherwise saury remains in the KR.

From the MW to the OY region: after 1st June, if KL is longer than 19.9 cm, saury migrate to the OY region irrespective of OY water temperature. If 9.9 cm < KL ≤ 19.9 cm, then saury migrate into the OY region when OY water temperature is higher than 9 °C. If KL ≤ 9.9 cm, saury migrate into the OY region when OY water temperature becomes higher than 13 °C. This means that longer saury can migrate northward earlier than shorter ones.

3.2.2. *Southward (spawning) migration (Fukushima, 1979)*

From the OY to the MW region (MW to KR): after 1st October (15th November), if 24.0 cm ≤ KL, saury migrate into the MW (KR) region when OY (MW) water temperature is lower than 18 °C. If 24.0 cm ≤ KL < 29.0 cm, saury migrate into the MW (KR) region when OY (MW) water temperature is lower than 15.5 °C. If KL is shorter than 24.0 cm, saury migrate into the MW (KR) region when OY (MW) water temperature is lower than 13 °C. In general, this means that longer saury can migrate southward earlier.

3.3. *Food selectivity*

The functions describing consumption of multiple zooplankton prey items by saury follow Rose et al. (1999)

$$C = C_r f_c(T) \tag{2}$$

$$C_r = \sum_{j=1}^{n} C_j \tag{3}$$

$$C_j = \frac{C_{MAX}(PD_{ij} v_{ij}/K_{ij})}{1 + \sum_{k=1}^{n}(PD_{ik} v_{ik}/K_{ik})} \tag{4}$$

$$C_{MAX} = a_c W^{b_c} \tag{5}$$

where C is the total daily consumption (g prey g fish^{-1} day^{-1}), C_r the total daily consumption without the effects of temperature, $f_c(T)$ the temperature dependent function for

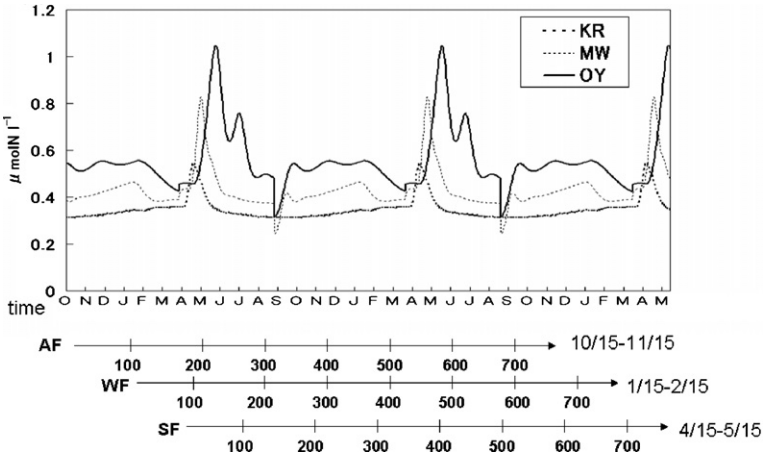

Fig. 4 – Model simulated seasonal variation of the total amount of food available to young and adult saury (stages 3–9 of Table 2) in the Kuroshio (KR), the mixed water (MW) and the Oyashio (OY) region. In the MW and the OY region, ZL + ZP is indicated and in the KR region, ZS + ZP is indicated. The vertical axis shows the prey density and the horizontal axes show time (months) and ages in days of AF, WF and SF, respectively.

consumption, T the seawater temperature (°C). j and k denote prey type, i denotes predator type (saury life stages), n the total number of prey items, C_j the consumption of prey j (corresponding to $j=1$ for ZS, $j=2$ for ZL and $j=3$ for ZP), C_{MAX} the maximum consumption rate (g prey g fish^{-1} day^{-1}), v_{ij} the vulnerability coefficients for predator i on prey j (dimensionless), K_{ij} the half saturation constant (g prey m^{-3}) for individual predator type i feeding on prey type k, and PD_{ij} is the density for prey type j (g prey m^{-3}). Eq. (5) includes the parameters a_c (the intercept for the allometric mass function) and b_c (the slope of the allometric mass function for consumption). More details can be found in Ito et al. (2007) and Megrey et al. (2007). The values of vulnerability and half saturation constants for each region are listed in Table 2 depending on the spawning season (Sugisaki and Kurita, 2004).

3.4. *Model simulations*

Similar to the control run of Ito et al. (2004), the saury bioenergetics/ecosystem coupled model was driven by idealized seasonal forcing. The idealized seasonal change of SST (Fig. 6a of Ito et al., 2004) was determined from the World Ocean Atlas 1998 (Antonov et al., 1998) and solar radiation forcing (Fig. 6b of Ito et al., 2004) was determined from the dataset of Oberhuber (1988). Under this idealized forcing, the mixed layer thickness showed clear seasonal variations in response to the seasonal change of SST (Fig. 6c of Ito et al., 2004). Following changes in the mixed layer thickness, the exchange rate between the mixed layer and the bottom layer also changed. As a result, nutrients supplied from the bottom layer were set by the seasonal forcing. In the mixed layer, phytoplankton used nutrients for photosynthesis under solar radiation forcing. Zooplankton biomass varied in response to the biomass changes in phytoplankton. Additionally, the seasonal vertical ontogenetic migration of ZL enhanced the seasonal variation of phytoplankton and other zooplankton biomass.

4. Results

Table 2 shows that larvae (stage 1) feed only on ZS. Juveniles (stage 2) feed on ZS and ZL in the MW and OY regions, and only ZS in the KR region because there is no simulated ZL in the KR region. Young and adult saury (stages 3–9) feed on ZL and ZP in the MW and OY region. In KR, because ZL are absent, saury feed not only on ZP but also on ZS to avoid starvation. In Fig. 4, the seasonal variation in the total food available (zooplankton biomass available) to young and adult saury is shown (i.e., in the MW and OY region, density = ZL + ZP and in the KR region, density = ZS + ZP). Food density was the highest in the OY region (Fig. 4), especially during summer. This means that saury grow faster the earlier they enter the OY.

The time dependent growth of Pacific saury with three different birth dates (Fig. 5) showed that autumn-spawned fish (AF) and winter-spawned fish (WF) grew more quickly than spring-spawned fish (SF) in the first year. The body weight of the AF and WF decreased in first year's winter (for AF, from

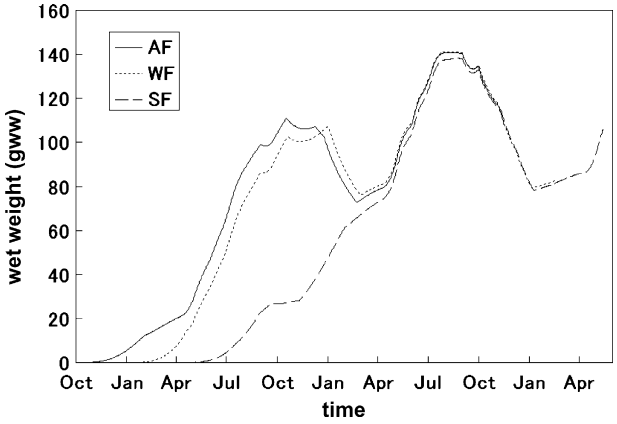

Fig. 5 – Model simulated time dependent change in wet weight of autumn (AF), winter (WF) and spring (SF) spawned saury, respectively.

10th December to 23rd February, for WF from 30th December to 27th February) because of spawning. However, the body weight of SF did not decrease in the first year because they could not grow quickly reach the required weight (i.e. 71 g which corresponds to KL > 25 cm) to spawn within 1 year (see Figs. 3 and 5). The time-varying growth rate of each fish (the origin is the date from each birth date) together with the ambient temperature is shown in Fig. 6. Below we describe the details related to the simulated temporal dynamics.

Age in days 1–100: WF growth rate was higher than AF and SF. Since the spring bloom occurred early in the KR region, only WF was able to use the high zooplankton (ZS) densities sustained by the April spring bloom (not shown) and growth of WF was the fastest. AF and SF were in the MW region and the seawater temperature was too low for AF (the last half of stage 1) and SF (the first half of stage 1). The optimal temperature is 20–26 °C for larvae (stage 1) and 16–20 °C for juvenile, young and adult saury (stages 2–9).

Age in days 100–130: WF growth rate was higher than AF and SF. WF migrated into the MW region matching the spring bloom and was able to use high prey density (ZS and ZL). AF was in the KR region and had few prey to consume, whereas,

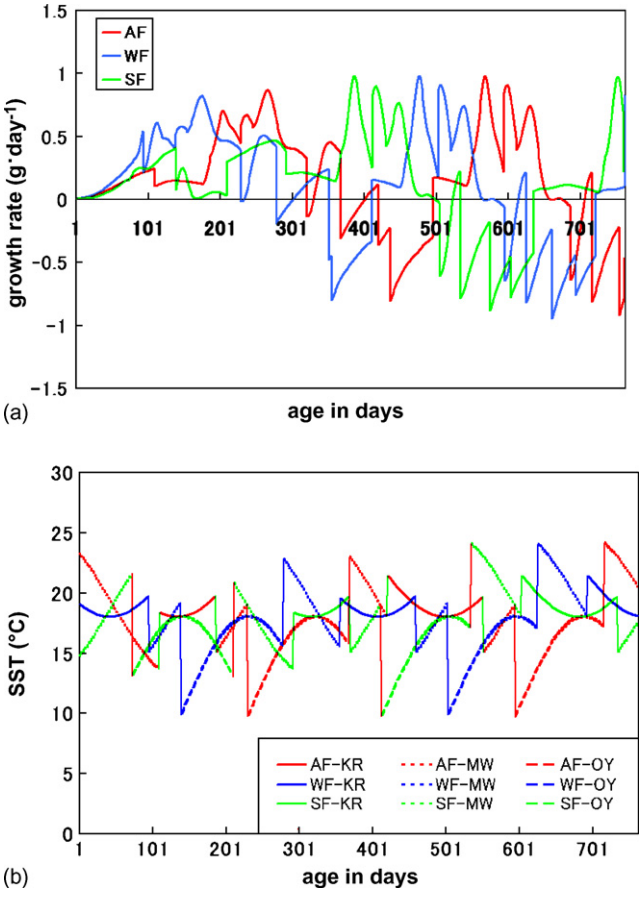

Fig. 6 – Model simulated (a) the time-varying growth rate of autumn (AF), winter (WF) and spring (SF) saury, respectively, and (b) the ambient water temperature. KR, Kuroshio region; MW, mixed water region; OY, Oyashio region. For instance, AF-KR means autumn-spawned fish in the Kuroshio region.

SF was in the OY region but the prey density was not high because it was August (not shown).

Age in days 130–200: WF showed the highest growth, followed by AF and SF. WF migrated into the OY region and prey density was high because it was June (Fig. 4), while AF was still in the KR region. SF was also in the OY region but the prey density was not high relative to the WF case since it was September–October (Fig. 4).

Age in days 200–280: AF showed the highest growth, followed by SF and WF. AF migrated into the MW and OY regions and encountered high prey density sustained by the spring bloom. AF migrated into the MW region and seawater temperature was optimal for AF growth. WF was in the OY region but prey density was not high because it was August–October (Fig. 4).

Age in days 280–350: AF and SF growths were higher than WF. AF was still in the OY region and food availability was high. However, in the middle of this period (September for AF), AF growth rate decreased rapidly because the disappearance of ZL in the OY region resulted in a rapid decrease in prey density (Fig. 4). SF migrated into the KR region and the prey density was not high compared to the prey density in the MW region from January to March (Fig. 4). WF was in the MW region and in the beginning half of this period the seawater temperature was too high, hence growth rate was very low.

In this period, WF and AF lost weight by spawning (starting on day 350 for WF and on day 420 for AF) while SF did not loose weight until day 510, which means it does not spawn until age 1.

Age in days 350–500: SF growth rate was higher than WF and AF. SF moved into the MW and OY regions and the prey density was very high because it was April–August (Fig. 4). SF started a second northward migration earlier (day 380) than WF (day 550) and AF (day 720). Conversely WF and AF growth rates decreased rapidly and became negative because they matured sufficiently and spawned eggs.

Age in days 500–600: WF and AF growths were higher than SF. WF and AF moved into the MW and OY regions and prey density was very high because the migration timing was June–August for WF and March–May for AF (Fig. 4). Conversely SF growth rate decreased rapidly because of first spawning.

Age in days 600–730: SF growth rate was higher than WF and AF. SF growth rate changed from negative to positive after spawning. Conversely WF and AF growths decreased rapidly because of their second spawning.

The histograms in Fig. 7 represent the size distribution of fished Pacific saury (Kosaka, 2000). Our simple model (left hand side of Fig. 7) could explain the bimodal size structure of landed fish (i.e., from September to November two peaks can be seen, and in December they become one). For example, in September age-1 saury of all three spawned cohorts showed larger sizes (31.5 cm), whereas, age-0 saury of AF and WF showed intermediate sizes (28 and 26.5 cm) and SF showed smaller sizes (18 cm). On the other hand, the observed size composition shows two peaks of cohorts at 31–32 and 26–27 cm. The 31–32 cm size roughly corresponds to modeled age-1 saury and the 26–27 cm size roughly corresponds to modeled saury size of age-0 AF and WF. Moreover, the size of age-0 SF (18 cm) is observed as the smaller edge of the size distribution. In December age-1 saury of WF and SF migrated

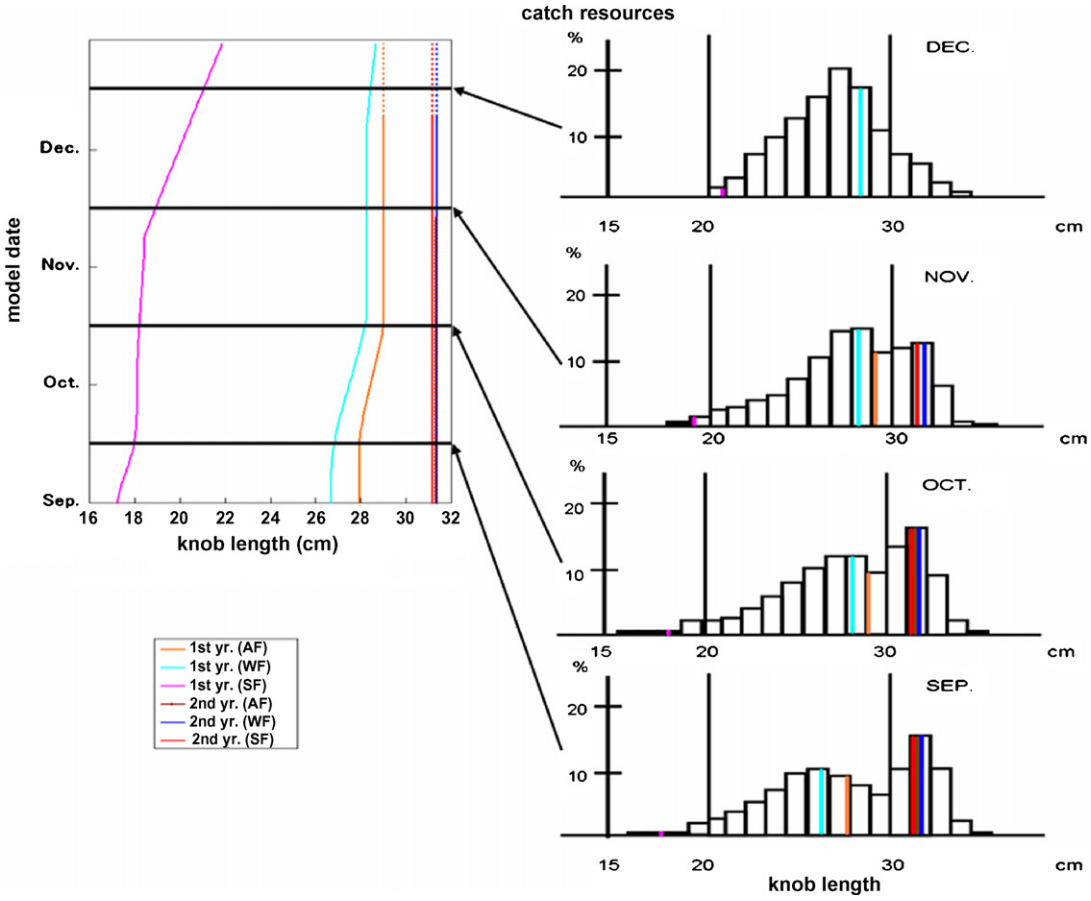

Fig. 7 – The left hand side figure shows that model simulated knob length of each fish during the fishery season. The vertical axis shows model date and the horizontal axis shows knob length (cm). The solid lines mean saury in the MW or the OY region and they are considered as commercial resources. The broken lines mean saury in the KR region and they are not considered commercial resources because the main fishery grounds are found in the MW and the OY region and not in the KR region. The "1st yr." means saury appear in the first year commercial fishery as age-0 fish and the "2nd yr." means saury appear in the second year commercial fishery as age-1 fish. The right hand side histograms show monthly mean knob length from fisheries landing data (Kosaka, 2000). The vertical axis shows the percentage of the fishery catch resources and the horizontal axis shows knob length. The color bars in the right hand side figure correspond to the model simulated size distribution of Pacific saury.

to the KR region and they were not considered as commercial fish (broken lines of Fig. 7 (left)) because the main fishery grounds are in the MW and OY regions and not in the KR region. In addition, age-1 saury of AF disappeared because they reached the end of their life span. Age-0 saury of all three spawned cohorts grew larger and those of AF, WF and SF became 29, 28.5 and 21 cm, respectively. However, age-0 saury of AF migrated to the KR region and disappeared in the MW or OY regions and the observed size composition became unimodal centered at 27–28 cm. This peak roughly corresponds to modeled age-0 WF. The disappearance of the 31–32 cm peak seems to roughly correspond to modeled age-1 WF and the disappearance of SF in the MW or OY regions and the death of age-1 AF. Moreover, the size of age-0 SF (21 cm) is observed as the smaller edge of the size distribution. Therefore, we can conclude that our simple model reproduced the observed size distribution of Pacific saury in the fishery season.

5. Conclusion and discussion

A fish bioenergetics model coupled with an ecosystem model (NEMURO.FISH) was developed to explain the size structure of landed Pacific saury. Ito et al. (2004) adapted NEMURO.FISH to the coupled model and expanded it to three ocean boxes corresponding to the KR, OY, and MW region. In this box model, the temperature difference between SST and the bottom layer temperature determined the mixed layer depth and the nutrient exchange rate with the bottom layer. Because the bottom layer temperature was fixed, SST mainly determined variation in the lower trophic level ecosystem.

WF showed the fastest growth, and SF showed the slowest growth in the first year (Fig. 6a). In the second year, SF showed the fastest growth (the time to reach 120 g wet weight). Okuda (2002), which adapted the method of Kurita et al. (2004), also suggested that observational data show that spring-spawned

cohorts have the slowest growth in the first year. Moreover, they suggested that winter-spawned cohorts show the highest growth in earlier stages, then winter-spawned cohorts catch up with autumn-spawned cohorts in wet weight and KL by the first winter. Spring-spawned cohorts catch up with autumn-spawned cohorts and winter-spawned cohorts in wet weight and KL by the second early summer. Spring-spawned cohorts spawn only in the second winter while autumn and winter-spawned cohorts spawn both in the first and second winter. These observational results correspond well with our model results (see Fig. 5). Why did SF show the fastest growth in the second year in spite of the slowest growth in the first year? There are two reasons: first, SF did not spawn during their first year (not shown). On the other hand, WF and AF spawned during their first year (not shown) and therefore experienced weight loss due to spawning. Second, SF started their northward migration earlier (Fig. 6b), found themselves in better feeding conditions and quickly gained in length and weight in the second year. This difference in growth, which depends on the spawning season, can explain the bimodal size distribution in the early autumn catch data and the unimodal distribution in the December size distribution catch data (Fig. 7). Fig. 7 shows the importance of WF resources because the size composition of modeled WF (both age-0 and age-1) corresponds with the bimodal characteristic of the observed early autumn size composition data. Moreover, in December, the observed size distribution becomes unimodal and modeled age-0 WF corresponds to this peak. The death of modeled age-1 AF and age-1 SF and WF migrations into the KR region roughly correspond to the disappearance of the observed larger size mode. According to Kurita (2001), saury spawning is intensified in winter. This winter intensification might cause the WF population to be larger than any other season spawned fish so that a large WF population corresponds to the peaks of the observed size composition (right hand side of Fig. 7). However our simple model is a bioenergetics model and we are unable to estimate the numbers in the saury population. To extend this work, we should consider a population dynamics model.

We recommend making greater efforts to collect observational data on all saury life-stages to better parameterize models such as NEMURO.FISH. Models like NEMURO.FISH can be very useful to analyze the mechanisms governing changes in fish growth. However, additional work in determining certain key parameters for Pacific saury still remains to be completed. The difficulty of rearing saury in the laboratory has slowed the potential improvement of modeling efforts for saury (i.e., the accuracy and precision of model parameters). Incubation laboratory experiments on all saruy life stages aimed to estimate or validate the most important consumption and respiration parameters (see Megrey et al., 2007) required by NEMURO.FISH, should be continued. Information during young life stages are insufficient and this life stage exists mainly in the MW region, a key area in the model (Ito et al., 2004).

Though Ito et al. (2004) showed the importance of SST effects in the MW region, Tian et al. (2000) pointed out the importance of winter time SST in the Kuroshio extension region and north of the MW region. This discrepancy may occur because Tian et al. (2000) analyzed an abundance index derived from historical fish landing data, which included information on weight and also number. When considering changes in the biomass of Pacific saury, variation in both the weight and number must be taken into consideration. Megrey et al. (2007) recognized this problem and described a full implementation of NEMURO.FISH that merges a population dynamics model tracking numbers in time with a fish bioenergetics/ecosystem coupled model tracking changes in weight in time. This kind of model will be extremely relevant for fisheries management issues.

Acknowledgements

We would like to thank Dr. K. Okuda VENFISH project leader, all colleagues of VENFISH project team, Drs. M. Terasaki, H. Sugisaki and Y. Sakurai for their many useful information, discussion and suggestions.

REFERENCES

Antonov, J., Levitus, S., Boyer, T.P., Conkright, M., O'Brien, T., Stephens, S., 1998. World Ocean Atlas 1998: Temperature of the Pacific Ocean, vol. 2. NOAA Atlas NESDIS 28: US Government Printing Office, Washington, DC, 166 pp.

Fukushima, S., 1979. Synoptic analysis of migration and fishing condition of saury in the Northwest Pacific ocean. Bull. Tohoku Reg. Fish. Res. 41, 1–70 (in Japanese).

Ito, S., Kishi, M.J., Kurita, Y., Oozeki, Y., Yamanaka, Y., Megrey, B.A., Werner, F.E., 2004. Initial design for a fish bioenergetics model of Pacific saury coupled to a lower trophic ecosystem model. Fish. Oceanogr. 13, 111–124.

Ito, S., Megrey, B.A., Kishi, M.J., Mukai, D., Kurita, Y., Ueno, Y., Yamanaka, Y., 2007. On the interannual variability of the growth of Pacific saury (*Cololabis saira*): a simple 3-box model using NEMURO. FISH. Ecol. Modell. 202, 174–183.

Kishi, M.J., Kashiwai, M., Ware, D.M., Megrey, B.A., Eslinger, D.L., Werner, F.E., Aita, M.N., Azumaya, T., Fujii, M., Hashimoto, S., Huang, D., Iizumi, H., Ishida, Y., Kang, S., Kantakov, G.A., Kim, H.-C., Komatsu, K., Navrotsky, V.V., Smith, S.L., Tadokoro, K., Tsuda, A., Yamamura, O., Yamanaka, Y., Yokouchi, K., Yoshie, N., Zhang, J., Zuenko, Y.I., Zvansky, V.I., 2007. NEMURO—Introduction to a lower trophic level model for the North Pacific marine ecosystem model. Ecol. Modell. 202, 12–25.

Kosaka, S., 2000. Life history of the Pacific saury *Cololabis saira* in the northwest Pacific and consideration on resource fluctuations based on it. Bull. Tohoku Natl. Fish. Res. Inst. 63, 1–96 (in Japanese).

Kurita, Y. 2001. Seasonal variability of spawning grounds and biomass of Pacific saury. Annual Report of the Research Meeting on Saury Resources 49, 203–205.

Kurita, Y., Nemoto, Y., Hayashizaki, K., Ida, H., 2004. Variation in patterns of daily changes in otolith increment widths of 0+ Pacific saury, *Cololabis saira*, off Japan by hatch date in relation to the northward feeding migration during spring and summer. Fish. Oceanogr. 13, 54–62.

Kurita, Y., 2006. Regional and interannual variations in spawning activity of Pacific saury *Cololabis saira* during northward migration in spring in the north-western Pacific. J. Fish Biol. 69, 846–859.

Megrey, B.A., Rose, K.A., Klumb, R.A., Hay, D.E., Werner, F.E., Smith, L.S., 2007. A bioenergetics-based population dynamics model of Pacific herring (*Clupea pallasii*) coupled to a lower

trophic level nutrient-phytoplankton-zooplankton model: description, calibration and sensitivity analysis. Ecol. Modell. 202, 144–164.
Oberhuber, J.M., 1988. An atlas based on 'COADS' data set. Tech. Rep. Max-Planck-Inst. Meteorol. 15.
Odate, S., 1977. On the distribution of Pacific saury in the North Pacific ocean. Res. Inst. North Pac. Sp. vol. 10, Fish., Faculty of Fisheries, Hokkaido University, Hakodate, Japan, 353–382 (in Japanese).
Okuda, K., 2002. Research projects on the prediction of fish populations by Fisheries Research Agency. II. VENFISH/results about walleye pollock and Pacific saury. Nippon Suisan Gakkaishi 68, 784–787 (in Japanese).
Oozeki, Y., Watanabe, Y., 2000. Comparison of somatic growth and otolith increment growth in laboratory-reared larvae of Pacific saury, *Cololabis saira*, under different temperature conditions. Mar. Biol. 136, 349–359.
Oozeki, Y., Watanabe, Y., Kitagawa, D., 2004. Environmental factors affecting larval growth of Pacific saury, *Cololabis saira*, in the Northwestern Pacific ocean. Fish. Oceanogr. 13, 44–53.
Rose, K.A., Rutherford, E.S., McDermot, D.S., Forney, J.L., Miles, E.L., 1999. Individual-based model of yellow perch and walleye populations in Oneida Lake. Ecol. Monogr. 69 (2), 127–154.
Sugisaki, H., Kurita, Y., 2004. Daily rhythm and seasonal variation of feeding habit of Pacific saury (*Colorabis saira*) in relation to their migration and oceanographic conditions off Japan. Fish. Oceanogr. 13, 63–73.
Suyama, S., Sakurai, Y., Shimazaki, K., 1996. Age and growth of Pacific saury *Cololabis saira* (Brevoort) in the Western North Pacific ocean estimated from daily otolith growth increments. Fish. Sci. 62, 1–7.
Suyama, S., Kurita, Y., Ueno, Y., 2006. Age structure of Pacific saury *Cololabis saira* based on observations of the hyaline zones in the otolith and length frequency distributions. Fish. Sci. 72 (4), 742–749.
Tian, Y., Akamine, T., Suda, M., 2000. Long-term variability in the abundance of Pacific saury in the northwestern Pacific ocean and climate changes during the last century. Bull. Jpn. Soc. Fish. Oceanogr. 66, 16–25 (in Japanese).
Watanabe, Y., Lo, N.C.H., 1989. Larval production and mortality of Pacific saury, *Cololabis saira*, in the northwestern Pacific ocean. Fish. Bull. U.S.A. 86, 601–613.
Watanabe, Y., Oozeki, Y., Kitagawa, D., 1997. Larval parameters determining preschooling juvenile production of Pacific saury (*Cololabis saira*) in the Northwestern Pacific. Can. J. Fish. Aquat. Sci. 54, 1067–1076.